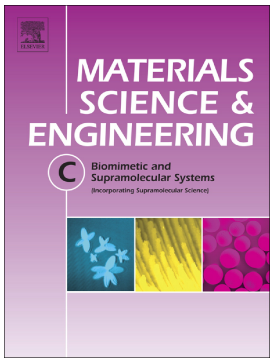

Biomechanical performance of hybrid electrospun structures for skin regeneration

J.R. Dias, S. Baptista-Silva, A. Sousa, A.L. Oliveira, P.J. Bártolo, P.L. Granja

PII: S0928-4931(18)30794-X
DOI: doi:10.1016/j.msec.2018.08.050
Reference: MSC 8844

To appear in: *Materials Science & Engineering C*

Received date: 16 March 2018
Revised date: 3 August 2018
Accepted date: 22 August 2018

Please cite this article as: J.R. Dias, S. Baptista-Silva, A. Sousa, A.L. Oliveira, P.J. Bártolo, P.L. Granja , Biomechanical performance of hybrid electrospun structures for skin regeneration. Msc (2018), doi:10.1016/j.msec.2018.08.050

Biomechanical performance of hybrid electrospun structures for skin regeneration

J.R. Dias[1,2,3,4*], S. Baptista-Silva[5], A. Sousa[1,3], A.L. Oliveira[5], P. J. Bártolo[7], P.L. Granja[1,3,4,6]

[1] i3S - Instituto de Investigação e Inovação em Saúde, Universidade do Porto, Porto, Portugal
[2] Centre for Rapid and Sustainable Product Development (CDRsp), Polytechnic Institute of Leiria, Leiria, Portugal
[3] INEB - Instituto de Engenharia Biomédica, Universidade do Porto, Porto, Portugal
[4] ICBAS - Instituto de Ciências Biomédicas Abel Salazar, Universidade do Porto, Porto, Portugal
[5] CBQF - Center for Biotechnology and Fine Chemistry, School of Biotechnology, Portuguese Catholic University, Porto, Portugal
[6] Faculdade de Engenharia da Universidade do Porto (FEUP), Porto, Portugal
[7] School of Mechanical, Aerospace and Civil Engineering & Manchester Institute of Biotechnology, University of Manchester, UK

*Corresponding author at Biomaterials for Multistage Drug & Cell Delivery Group, Instituto de Investigação e Inovação em Saúde, Universidade do Porto, Rua Alfredo Allen, 208, 4200-135 Porto, Portugal . Phone number +351 220 408 800, Fax +351 226 094 567, e-mail address:jrdias.juliana@gmail.com

Abstract

Wound dressings made by electrospun nanofibers have been demonstrating great potential to regenerate skin tissue as compared to the conventional membrane products available in the market. Until today most of the developed dressings have only demonstrated the capability to regenerate the dermis or epidermis. In this study we propose new hybrid electrospun meshes combining polycaprolactone and gelatin. Several approaches, multilayer, coating and blend were stablished to investigate the most appropriate hybrid structure with potential to promote skin regeneration in its full thickness. The structures were evaluated in terms of physico-chemical properties (porosity, water vapour permeability, contact angle and swelling degree) and according to its mechanical and biological performance. Multilayer and blend structures demonstrated to fit most of native skin requirements. However, looking to all the performed characterisation we considered multilayer as the most promising hybrid structures, due its high porosity which contributed to an ideal water vapour permeability rate and good mechanical and biological properties. Based on this multilayer structure is a promisor wound dressing.

Keywords: Hybrid structures; electrospun meshes; wound dressings; ECM; skin regeneration.

1. Introduction

The largest vital organ in the body is the skin. It represents 7% of its total weight, being its main function to protect the human being against the external environment [1-5]. This layered tissue plays other important functions such as the control of the body temperature, sense of touch or the synthesis of vitamin D [1, 6]. When skin damage occurs a consecutive cascade of events takes place to restore the skin structure and function [7, 8].This is known as wound healing, a process that consists, mainly in five different phases: haemostasis, inflammation, migration, proliferation and maturation, occurring sequentially after damage [7, 9]. Through this elaborate process the skin presents self-regeneration ability, although this capacity is strongly reduced in the case of full-thickness lesions, requiring for the use of a graft or dressing [4]. Despite the encouraging recent developments of new wound dressings and tissue engineering-based products, there is plenty of room for innovative strategies to promote skin tissue regeneration [10, 11]. Important advances have been made clinically with the use of PermaDerm® (Regenicin Inc., USA) and Apligraf® (Novartis, USA) [12], but a skin equivalent, able to fully replicate the important aspects of its functionality is yet to be developed. Last year a new promising wound dressing became available on the market, the MIRRAGEN™ Advanced Wound Matrix (ETS Wound care, USA) is based on fibrous borate bioactive glass and clinical trials demonstrated highly effective in diabetic ulcer patient's treatment. Over the last years electrospun meshes are have gained increasing attention through the combination of materials and processing strategies, which present great potential for skin regeneration [3].This year was certified the first company (Bioinincia, Spain) with the capability to scale up electrospinning technique for biomedical applications representing a great advance to materialise the research developed in this field [13]. Wound dressings prepared from electrospun nanofibers have been claimed to present exceptional properties compared to conventional dressings, such as improved promotion of haemostasis, absorption of

wound exudates, adequate permeability, conformability to the wound, and avoidance of scar induction [9, 14-16]. The skin multilayer structure, with a mesh-like organization, can be mimicked by electrospinning technology [11]. New electrospinning processing strategies are thus being explored in which natural and synthetic materials are combined with new design approaches allowing the production of hybrid structures [11]. Several research works explored the development of hybrid structures combining different fibre diameters [17-19], different materials to improve the properties of the structure [20-22] or combining aligned/random fibres [23]. For skin regeneration most of the available works only explore the combination of materials and different fibre diameters, building structures without gradients [11].

In this work we propose to combine the advantages of natural (gelatin) and synthetic (polycaprolactone) polymers into electrospinned nanofibers through different approaches to investigate the most suitable structure to promote skin regeneration. Polycaprolactone (PCL) is a well-known aliphatic linear polyester that has been extensively used in tissue engineering applications due to its biodegradability, biocompatibility, structural stability and mechanical properties [24, 25]. PCL presents semi-crystalline structure, hydrophobic nature and low bioactivity which reduces the cell affinity and small tissue regeneration rates [26, 27]. To overcome these drawbacks we introduced into the structure gelatin (Gel), which is obtained through the collagen denaturation and is typically derived from bovine or porcine skin [28, 29]. Due to its biological origin, Gel is similar to collagen and apparently is able to retain signals information such as the arginine–glycine–aspartic acid (RGD) sequence [12]. It also promotes differentiation and proliferation, which makes it an attractive polymer for tissue engineering [30-32]. Despite the similarity of Gel with collagen, it presents better tensile modulus and possess excellent biodegradability, non-antigenicity, and cost efficiency as collagen [28, 33]. One of the major drawbacks of Gel is that it dissolves as a colloidal solution at temperatures at 37 °C or above, and gels near room temperature

[30, 34]. As such, Gel electrospun meshes are often cross-linked or combined with synthetic polymers in order to maintain a fibrous structure [35, 36].

Here we explore three different processing strategies, multilayer, coating and blend to combine both materials into hybrid wound dressing structures capable of promoting skin regeneration. The main goal is better mimic the skin ECM not only in morphological point of view but, also, its mechanical and biological properties.

2. Materials and Methods

2.1 Materials & Methods

PCL (Mw 50000 (g/mol), bulk density: 1.1g.cm-3) was kindly supplied by Perstorp (Malmo, Sweden) and dissolved in acetone (DMK) that was purchased to Sigma-Aldrich (Missouri, USA). Gel powder of pig skin (type A, 300 bloom, 60 mesh) were kindly supplied by Italgelatine (Santa Vittoria d'Alba, Italy), and the acetic acid glacial (AA) was purchased from PanReac AppliChem (Barcelona, Spain). To increase the conductivity of Ge/AA solution was added 2% v/v of triethylamine (TEA) purchased to Sigma-Aldrich (Missouri, USA). 1,4-butanediol diglycidyl ether (BDDGE) was provided from Alpha Aesar (Massachesetts, USA) and used as crosslinking agent of Gel without any further purification. A Gel/AA/TEA solution (15 wt-%) and PCL/DMK (17wt-%) was prepared for electrospinning by dissolving the polymers and stirred it at 37ºC overnight. The crosslinker was added and stirred immediately before the electrospun fibers' production. To the preparation of the blend solution PCL and Ge were dissolved in AA and TEA (2 % v/v), (17 wt-% and 15 wt-%, respectively) and was stirred together during 2h before the production of the meshes. No crosslinker agent was added due the hydrogen bonds formed between materials which stabilized Gel in aqueous solution [37].

Pure PCL and Gel meshes have been used as controls. Gel was *in situ* crosllinked with BDDGE according to our previous developed work [38].

2.2 Electrospun meshes preparation

Polymeric nanofiber meshes were processed by using a specially designed electrospinning machine using a single jet approach. Control samples were produced with pure PCL and Gel while the hybrid structures resulted from a combination of both polymers using three distinct methodologies. The multilayer structure was composed by 5 layers combining the materials (Gel/PCL/Gel/PCL/Gel). The 5 layers was defined in order to obtain a compact structure (with no physical separation between layers). The second reason was to guarantee that, independently of side (top or bottom), the first contact between the multilayer structure and cells occurs always with the same material. The blend mesh was produced after mixing both polymers in solution followed by spinning into one single fibre to obtain a filament that combined both materials and consequently obtain combined properties. Finally, we have used coating methodology which consisted in the electrospinning of a PCL fibre mesh production followed by immersion in a Gel solution (5% w/v) and drying at 37 ºC. The details regarding the different processing parameters are available in Table 1. The optimal processing parameters of PCL and Gel electrospun mesh were defined in previous work [39].

All the non-woven electrospun meshes were obtained at room temperature and relative humidity of 40-50% using a syringe pump (SP11Elite, Harvard Apparatus, Massachusetts, USA) combined with a high voltage source (HV power supply, Gamma High Voltage Research, Florida, USA) and a grounded copper plate as collector. Crosslinking of electrospun Gel fibers was carried out through the incorporation of BDDGE on Gel solution to avoid the loss of configuration that is usually induced by immersion in the crosslinking solution [38, 40].

Table 1. Processing parameters and after processing.

Electrospun mesh	Flow rate (mL/h)	Distance between collector and needle tip (cm)	Voltage (kV)	After processing
PCL	3.17	12	10	none
Gel	0.4	12	11	Incubation at 37ºC, during 72h
Multilayer	5 layers structure (Gel-PCL-Gel-PCL-Gel)			Incubation at 37ºC,

				during 72h
Coated	3.17	12	10	Immersion in a Gel solution during 30 min followed by incubation at 37ºC, during 72h
Blend	0.3	12	11	None

2.3. Physicochemical characterization

2.3.1. Apparent density and porosity

The apparent density and porosity of electrospun meshes were calculated using equations (1) and (2) [41], respectively, where the mesh thickness was measured using a micrometer.

$$\text{Apparent density } \left(g \cdot cm^{-3}\right) = \frac{\text{mesh mass(g)}}{\text{mesh thickness (cm)} \cdot \text{mesh area (cm}^2\text{)}} \quad (1)$$

$$\text{Mesh porosity} = \left(1 - \frac{\text{Mesh apparent density(g} \cdot \text{ cm}^{-3}\text{)}}{\text{Bulk density of PCL/Gel(g} \cdot \text{ cm}^{-3}\text{)}}\right) \cdot 100\% \quad (2)$$

2.3.2. Morphology and fiber diameter

The morphology of each electrospun fibrous mesh was examined by scanning electron microscopy (SEM) using a Quanta 400 FEG ESEM/EDAX Genesis X4M (FEI Company, Oregon, USA). Prior to examination samples were coated with a gold/palladium (Au/Pd) thin film, by sputtering, using the SPI Module Sputter Coater equipment (SPI Supplies, Pennsylvania, USA). SEM images were also used to evaluate the fiber diameter distribution using Image J software. To each condition three individual samples were analyzed and fifty measurements per image were carried out.

2.3.3. Structure

Fourier transform infrared (FTIR) spectroscopy with attenuated total reflectance (ATR) was used to evaluate the chemical composition of the materials and to detect possible structural changes. FTIR analyses were carried out using an Alpha-P Brucker FTIR-

ATR spectrometer (Brucker, Brussel, Belgium), in the range of 4000–500 cm^{-1}, at a 4 cm^{-1} resolution with 64 scans.

2.3.4. Water uptake

To assess dissolvability samples were dried for 24h before weight determination, after which they were incubated in distilled water and sodium azide (0.02%) as bacteriostatic agent. After 24h of incubation samples were removed from the distilled water solution and weighted again to evaluate the swelling degree (eq. 4).

$$\text{Degree of sweeling } (\%) = \frac{W_w - W_d}{W_d} \cdot 100, \quad (4)$$

where W_w is the wet weight and W_d is the dry weight.

2.3.5. Water vapor permeability

The water permeation rate of electrospun meshes was estimated. Glass bottles with the same size and type were filled with PBS solution and the electrospun meshes were fixed on their openings. The area available for vapor permeation was 2.39 cm^2. Evaporation of water through the mesh was monitored by the measurement of weight loss according to standard test methods for water vapor transmission [42]. Briefly, each set was weighted and kept at 32°C during 24h, after which the weight of each set was recorded again to quantify the amount of water evaporated.

2.3.6 Contact Angle

To assess the hydrophilicity of electrospun samples a static contact angle through optical contact angle was used (Data Physics, model: OCA 15 plus, Filderstadt, Germany). The water contact angle was measured through the spread of droplets on the surface and recording its height and width. Each experiment was recorded during 1 minute.

2.3.7 Mechanical properties

The tensile strength and modulus of electrospun samples were determined in wet state using a texturometer (TA.XT Plus model, Stable Micro System SMD, Surrey, UK) with a 5N load cell. Testing was carried out in a controlled environment at room temperature (RT) and relative air humidity of 45%. The gauge length was 15 mm and the test speed was 1 $mm{\cdot}s^{-1}$. At least five individual samples were tested from each group and measurements were reported as mean ± standard deviation according the statistical method used (mixed effect model). All experiments were performed with samples thickness prior perform the tensile tests.

2.4. *In vitro* studies

Human dermal neonatal fibroblasts (hDNF) isolated from the foreskin of healthy male newborns (ZenBio, North Carolina, USA) were cultured, expanded, and maintained in Dulbecco's modified eagle medium (DMEM) (Gibco, California, USA), at 37ºC in a humidified atmosphere of 5% CO_2. The culture medium was changed twice a week and cells were trypsinized (0.25% trypsin/0.05% ethylenediamine tetraacetic acid (EDTA)/0.1% glucose in phosphate buffered saline (PBS) (pH 7.5)) when they reached 70-80% of confluence. Cells from passages between 8 and 11 were used in this study.

2.4.1. Cytotoxicity

To evaluate their cytotoxicity electrospun meshes were tested in direct (samples) and indirect (leachables) contact under pre-washed in ultrapure water. Samples were sterilized into a vertical flow chamber using UV-C light with a wavelength of 270 nm followed by washing during 24h. hDNF cells were seeded in culture wells for 24h at a density of $2x10^4$ cells/well. 24h later, samples (direct contact) and culture medium having been in contact with samples (indirect contact) were incubated with the cells for another 24h. The culture medium was then removed from the wells and fresh basal medium with 20% v/v resazurin (Sigma-Aldrich, Missouri, USA) was added. Cells were incubated (37ºC, 5% v/v CO_2) for an additional 2h period, after which 300 μL per well were transferred to a black 96-well plate and measured (Ex at 530 nm, Em at 590 nm)

using a micro-plate reader (Synergy MX, BioTek, New Hampshire, USA). The control consisted in cells alone. To avoid the evaporation of cell culture medium during the experiments the analyses were performed using only the central wells, for that reason there are more than one control (one control per well-plate used).

For the quantification of the total double-stranded DNA (dsDNA) content, the cell pellets were recovered from wells and washed with phosphate buffered saline (PBS). The suspension was then centrifuged (10 000 rpm, 5 min) and then stored at -20ºC until further analysis. The dsDNA quantification was performed using the Quant-iT PicoGreen dsDNA kit (Molecular Probes, Invitrogen, California, USA), according to the manufacturer's protocol. Briefly, the samples were thawed and lysed in 1% v/v Triton X-100 (in PBS) for 1h at 250 rpm at 4ºC. Then, they were transferred to a black 96-well plate with clear bottom (Greiner, Kremsmunster, Austria) and diluted in Tris-EDTA buffer (200 mM Tris–HCl, 20 mM EDTA, pH 7.5). After adding the Quant-iT PicoGreen dsDNA reagent, samples were incubated for 5 min at RT in the dark, and fluorescence was measured using a microplate reader (Ex at 480, Em at 520 nm).

2.4.2. Cell metabolic activity and proliferation

Cell metabolic activity and proliferation assays were performed using hDNF cells seeded on electrospun meshes at a cell density of $1x10^4$ cells per sample. To promote an efficient cell penetration into the mesh the seeding was performed with only 10 μL and incubated for 2 hours. 500 μL was then added and cultured during 14 days, changing the medium every 3 days. The control consisted in samples without cells. Due to the dry cell culture medium during the experiments the analyses were performed using only the central wells, for that reason there are more than one control.

Metabolic activity was estimated using the resazurin-based assay and using electrospun meshes without cells as control. For the proliferation assay samples direct contact assay was performed with hDNF cells and pre-washed with ultrapure water.

Afterwards, they were cultured for 14 days, and their metabolic activity was measured at days 1, 3, 7 and 14.

2.4.3 Cell morphology, fibronectin deposition and Ki-67 expression

For the studied time-points (1 and 14 days) cells seeded in electrospun meshes were stained for filamentous actin (F-actin), nuclei (Dapi), fibronectin (FN) deposition and ki-67 protein expression (ki67). Briefly, samples were washed with PBS, fixed for 20 min in 4 wt-% paraformaldehyde (PFA, Sigma-Aldrich, Missouri, USA), and permeabilized with 0.2% Triton X-100 (Sigma-Aldrich, Missouri, USA) for 7 min. Samples were then incubated for 1h with 1 wt-% bovine serum albumin (BSA, Merck, New Jersey, USA) in PBS. For FN staining, electrospun meshes were incubated overnight at 4ºC with rabbit anti-fibronectin (f3648, Sigma-Aldrich, Missouri, USA, 1: 300) and then with the goat anti-rabbit secondary antibody Alexa Fluor® 488 F(ab')$_2$ fragment (Molecular Probes-Invitrogen, California, USA, 1: 2000, 2 h at RT). After this, samples were incubated with the conjugated probe phalloidin/Alexa Fluor® 594 (Molecular Probes-Invitrogen, California, USA, 1: 40, 1 h at RT) for F-actin staining. For ki67 staining, electrospun meshes were incubated overnight at 4ºC with rabbit anti-ki67 (Ab15580, Abcam, Cambridge, UK, 1: 200) and then with the goat anti-rabbit secondary antibody Alexa Fluor® 488 F(ab')$_2$ fragment (Molecular Probes-Invitrogen, California, USA, 1: 1000, 2 h at RT). In both staining samples were subsequently washed three times with the PBS solution and nuclei were counterstained with 40,6-diamidino-2-phenylindole dihydrochloride (DAPI, Sigma-Aldrich, Missouri, USA, 0.1 $mg \cdot mL^{-1}$) in vectashield (Vector laboratories, California, USA), just before confocal visualization (CLSM, Leica SP2AOBS, Leica Microsystems, Wetzlar, Germany) using LCS software (Leica Microsystems, Wetzlar, Germany). The scanned Z-series were projected onto a single plane and pseudo-colored using ImageJ. The cells cultured in electrospun meshes were also visualized trough SEM to evaluate their morphology. Briefly, samples were

washed with PBS, fixed for 30 min in 2.5 wt% glutaraldehyde (GA) (Fluka, Seelze, Germany), and dehydrated with a successive graded ethanol series (40, 50, 70, 90 and 100%) for 15 min each. After that, critical point drying (CPD7501, Polaron Range) was performed to ensure the complete dehydration of samples.

2.5. Statistical analyses

All data points were expressed as mean ± standard deviation (SD). Statistical analysis (Levene's and T test) was carried out using IBM SPSS Statistics 20.0 with 99% confidence level for cytotoxicity assays. Linear mixed model (LMM) was used to test differences between the effects of composition in Young's Modulus, tensile strength at break and elongation at break. Composition was treated as a fixed factor and replication experiment was treated as a random factor to take into account possible heterogeneity of the samples in each set. Parameters' estimation was performed by lme package and multiple comparison adjustment was performed by mulcomp package from the R statistical software [43]. The results were considered statistically significant when $p \leq 0.05$ (*).

3. Results and discussion

3.1 Macroscopic and morphological characterization

Electrospun skin substitutes are demonstrating an increased potential to promote cellular attachment, growth and differentiation due the high surface area, high aspect ratio and high microporosity provided by the low fiber diameter structure [11, 44-46].

SEM morphological images of electrospun meshes for different methodologies and controls are shown in Fig. 1 (a-d). According to the SEM images, electrospun meshes obtained shows uniform random deposition with continuous filaments well defined without presence of beads. Depending on the methodology there are distinct average diameters that can be visualized in Table 2. For multilayer samples the average fiber diameter are 490 ± 330 nm, in which the standard deviation is high as consequence of

the average diameters corresponding to fibers from PCL and Gel and consequently the range of diameters is high. The coated methodology presents the fibers with highest diameters (2050 ± 700 nm) of methodologies as consequence of coating. After PCL electrospun preparation the Gel bath make Gel cover some filaments make it larger and fill some pores. With the blend methodology was possible obtain the smallest fibers diameters (199 ± 107 nm) even compared to the control meshes, 417 ± 165 and 339 ±91 corresponding to PCL and Gel, respectively.

The skin ECM fibers, composed of collagen, elastin and fibrillin fibers , are reported to exhibit diameters between 10 and 300 nm, and the minimum fiber diameter required for fibroblast adhesion and migration, and maximum interfiber distance that fibroblasts are able to bridge, have been described as approximately 10 and 200 nm [11, 47, 48].

According to the above mentioned equations (Equations 1 and 2) the theoretical values for the porosity of the electrospun produced meshes range between 97.32 ± 0.83 % (Coated) and 98.78 ± 0.33 % (Gel) (Table 2). In the case of the coated methodology the value is below of 98% since the fibers were coated with the gelatin. Comparing Gel and the other electrospun meshes (PCL, Multilayer and Blend) the porosity is similar between them (~98.5%).

Table 2. Properties of electrospun mesh structures.

Sample	Apparent density (g.cm $^{-3}$)	Porosity (%)	WVP (g/m^2/day)	Swelling degree (%)	Average fiber diameter (nm)	Contact angle (º) t=0s	Mechanical properties		
							Elastic Modulus (MPa)	Tensile Strength (MPa)	Elongation at break (%)
PCL	0.021 ± 0.003	98.11 ± 0.24	2365.50 ± 121.22	341.19 ± 68.34	417 ± 165	135.98 ± 6.62	5.41 ± 2.45	0.87 ± 0.37	219.97 ± 76.08
Gel	0.009 ± 0.002	98.78 ± 0.33	2292.69 ± 147.36	568.92 ± 67.28	339 ± 91	36.62 ± 15.83	0.31 ±0.15	0.04 ± 0.03	29.1 ± 11.60
Multilayer	0.017 ± 0.001	98.61 ± 0.04	2470.75 ± 171.34	354.87 ± 13.05	n.a.	101.58 ± 17.82	2.51 ± 0.71	0.34 ± 0.11	83.20 ± 14.84
Coated	0.033 ± 0.010	97.32 ± 0.83	1862.13 ± 182.58	149.29 ± 46.51	2050 ± 700	91.86 ± 5.25	7.47 ± 1.85	1.09 ± 0.13	64.13 ± 10.57
Blend	0.015 ± 0.003	98.80 ± 0.24	2466.57 ± 76.84	198.06 ± 33.05	199 ± 107	37.74 ± 17.82	4.61 ± 4.14	1.29 ± 1.24	69.40 ± 33.25

3.2 Physico-chemical and structural characterization

FTIR-ATR analysis was performed to evaluate any interaction between synthetic and natural polymer in the hybrid structures developed, using the “raw” meshes as control. The different spectra obtained are shown in Figure 1 g). PCL spectrum is characterized by the presence of several bands being the most common at 1720.7 cm^{-1}, corresponding to the C=O bond characteristic in esters. Between 750 and 1500 cm^{-1} we can observe some bands corresponding to a CH_2 groups of PCL chain. Lastly, it can be observed two bands with 2863.69 cm^{-1} and 2941.57 cm^{-1}, corresponding to the CH bond. The FTIR spectra of Gel shows pronounced bands in four different amide regions, specifically at 1700-1600 cm^{-1} corresponding to amide I, at 1565-1520 cm^{-1}, to amide II, at 1240-670 cm^{-1} to amide III, and at 3500–3000 cm^{-1} corresponding to amide A [49-53]. The absorption of amide I contains contributions from the C=O stretching vibration of amide group and a minor contribution from the C-N stretching vibration [49]. Amide II absorption is related to N-H bending and C-N stretching vibrations. Amide III presents vibrations from C-N stretching attached to N-H in-bending with weak contributions from C-C stretching and C=O in-plane bending [54]. In our FTIR results, corresponding to the hybrid electrospun meshes no chemical change was observed, being possible to detect the presence of both polymers in the same structure.

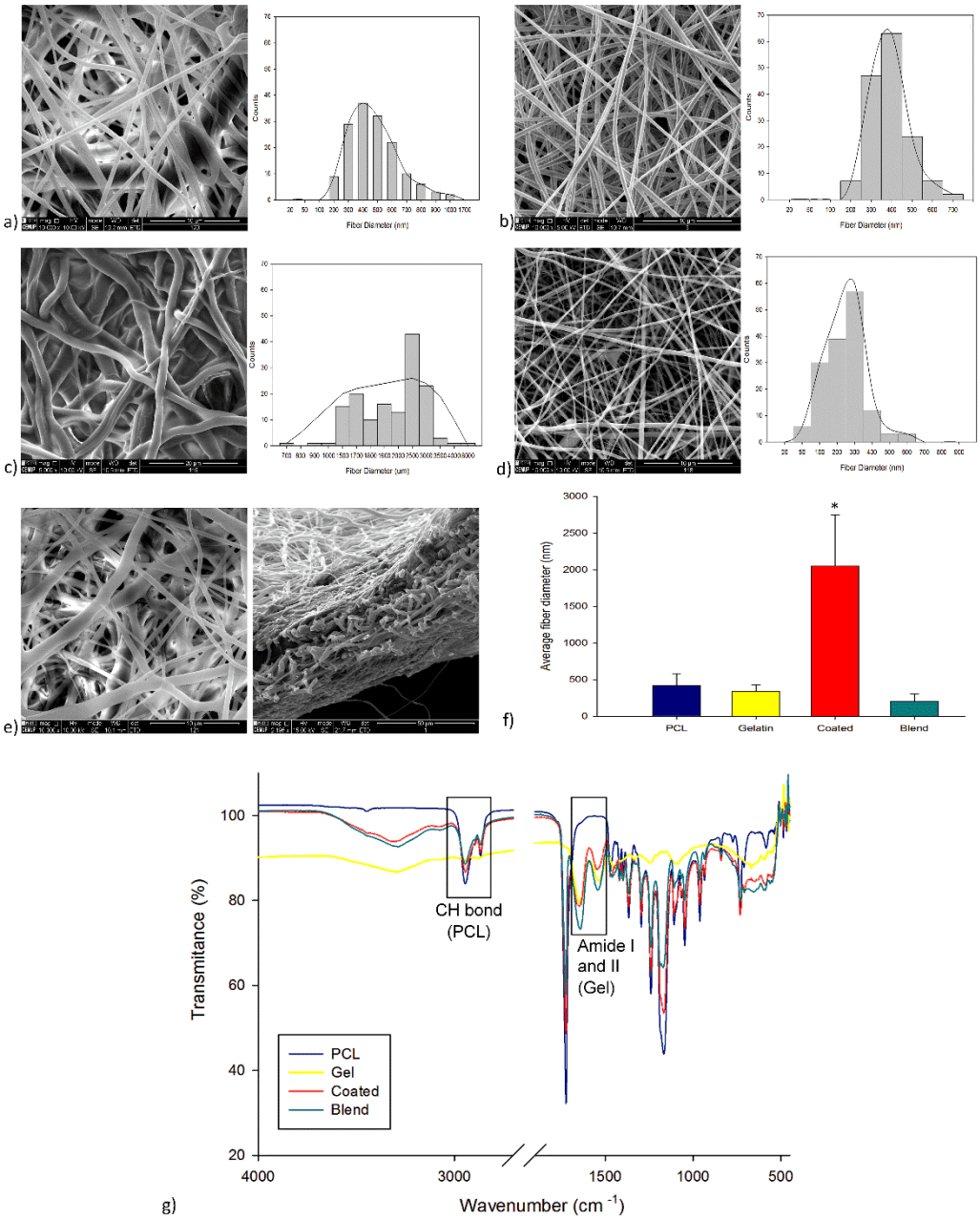

Figure 1. Scanning electron microscopy of hybrid structures and controls, a) PCL, b) Gel, c) Coated, d) Blend, e) Multilayer top and cross-section, f) comparative fiber average diameters, g) FTIR spectrums of electrospun meshes. Statistical significance for p≤0.05 (*).Scale bar: 10 µm.

The water uptake of biodegradable polymers indicates the hydrophilic/hydrophobic character of the materials and therefore, their susceptibility to degradation by hydrolysis processes [55]. To evaluate the hydrophilic character of the electrospun meshes, the contact angle between the meshes was measured by the sessile drop technique. As known, PCL has a hydrophobic character [56]. In agreement, nanofiber

meshes produced through electrospinning process presented an angle of 135.98 ± 6.62º (Table 2). On the other hand, Gel is characterized by its hydrophilic behaviour [57] and presented an angle of 36.62 ± 15.83º. The hybrid structures were, also, tested demonstrating a decrease of contact angle that are directly associated to the increase of hydrophilic character of sample through the incorporation of Gel. Due to the intrinsic characteristics of electrospun meshes after 30 seconds all sample absorbed the water droplet, being the values above corresponding to the two seconds of test. In fact, the high porosity allows for the penetration of water throughout the meshes even when is made by hydrophobic material.

One of the most important feature of a wound dressing is to control the water loss evaporation at an optimal rate. The dressing should be permeable to keep a moist environment and prevent wound dehydration [58]. However, it is important to emphasize that a moist wound environment is not a wet wound environment, since excess of exudates will lead the patient to hypergranulation tissue formation in the wound bed and macerated periwound skin [58, 59]. Therefore, an important objective in providing topical wound care is selecting a dressing which can maintain a moist wound surface while being able to remove the produced exudate [58-60]. A healthy skin presents a permeation of 204 g/m^2/day, while for injured skin, a first-degree burn, can range to 279 g/m^2/day and for a granulating wound to 5138 g/m^2/day [61, 62]. An ideal wound dressing must have a rate of 2500 g/m^2/day to provide an adequate level of moisture without compromising wound dehydration [58, 61, 63]. The permeability of water vapor through the electrospun meshes produced ranges from 1862.13 ± 182.58 (Coated) to 2470.75 ± 171.34 g/m^2/day (Multilayer). WVP is influenced by the pore size and interconnectivity between pores, small pores and packed fibers into the mesh decrease the permeability to the water vapor. The PCL mesh presents higher WVP than Gel. Despite the porosity of Gel being slightly higher the packing of fibers can be bigger due to lower diameter as compared to PCL fibers and for that reason the WVP is less than the PCL mesh. Looking to the hybrid structures, the Multilayer and Blend

methodologies presents values in the range of the ideal permeation rate, 2470.75 ± 171.34 and 2466.57 ± 76.84 g/m^2/day, respectively. However, the coated structure presents a WVP rate far from the ideal rate that is related to the lower porosity as compared to the other methodologies, consequence of coating with Gel that fill some pores.

The swelling degree of biodegradable polymers is correlated with its hydrophilic/hydrophobic character and, therefore, their susceptibility to degradation by hydrolysis processes [64]. The swelling increase the materials' flexibility and promotes changes in the dimensions of the implant material [65]. The processing methodologies have generated fiber meshes with distinct capabilities to uptake water. According to the swelling degree values shown in Table 2, Gel presents the higher swelling degree, consequence of its hydrophilic character. In spite of the hydrophobic character of PCL, it demonstrated a great capability to swell when processed into a nanofiber mesh. Coated structures have a swelling degree of 149.29 ± 46.51% which is the lowest value from all the processed fiber meshes, which is correlated with the fact that some pores were filled with gelatin limiting the water uptake. Regarding the Blend fiber meshes the swelling degree is also low compared to the other structures which can be related to the high packing of fibers due its low fiber diameter. The Multilayer structure presented the highest value of the hybrid meshes (354.87 ± 13.05%) because it combines, in the same structure, both materials in different layers which allows to keep the main characteristics of raw materials. In the same structure it was possible to increase the hydrophilicity and avoid the fiber packing due to the combination of fibers with a different range of diameters.

3.3 Mechanical properties

Electrospun meshes were investigated regarding to its mechanical performance, according to its different structure composition. Due to the heterogeneity of human skin, its mechanical properties presents a wide range of values. Can be considered as

reference values: 2.9-150 MPa for Young's Modulus, 1-32 MPa for Tensile Strength and 17-207 % for Elongation at break [66-69]. Representative stress-strain curves are shown in the Figure 2a), corresponding to the Young's Modulus (MPa), Elongation at break (%) and Tensile Strength at break (MPa). Besides improving the adequate environment for cells to adhere and proliferate, one of the most important reasons to combine PCL with Gel is to improve the poor mechanical properties of Gel [57], which is possible to observe in Figure 2. An important objective of this study is to evaluate which hybrid structure matches closely skin mechanical properties. Pure PCL and Gel meshes where used as controls, corresponding to the best and the worst mechanical properties, respectively. The main idea behind developing hybrid structures is to achieve intermediate properties and according the results (Fig. 2b), c) and d) and Table 2) it is notorious that the hybrid structures present improved properties (Young's modulus, Tensile strength at break and elongation at break) compared to pure Gel. The Young's Modulus of hybrid structures has not statistical significance when compared to the PCL, where PCL presents 5.41 ± 2.45 MPa, Multilayer 2.51 ± 0.71 MPa, Coated 7.47 ± 1.85 MPa and Blend 4.61 ± 4.14 MPa. Comparing the hybrid structures, the Multilayer and Coated show statistical significance, the last one presenting the higher elastic modulus even when compared to the PCL probably due to the lower porosity degree consequence of the coating on the PCL electrospun mesh that fill most of the pores and transform the mesh from high porosity to a membrane with low porosity. Some authors have been evaluating the effect of porosity and fiber diameter on mechanical properties and the results demonstrated that the porosity of the electrospun meshes has a greater effect on mechanical properties than fiber diameter. Meshes with low porosity, the elastic modulus is higher, due to the increased number of fibers/ amount of material in a unit cell contributed to the force on the meshes [70, 71].

The tensile strength at break (TSB) is based on the maximum tensile stress supported by the sample before break. The Coated and Blend samples show the high values of TSB measured from the different structures evaluated, followed by PCL, Multilayer and

Gel. Only the Blend structure presents statistical significance when compared to Multilayer and Gel electrospun meshes. Presents also a high standard deviation value related to the non-uniform elongation properties (PCL and Gel are randomly distributed inside of each fiber) that induces the defects started to appear at different positions of the sample [72].

Regarding to the elongation at break the PCL presents the highest value (219.97 ± 76.08 %) with statistical significance from other samples. Overall hybrid structures presented a better mechanical performance as compared to pure Gel.

According to the results, in terms of mechanical properties, all hybrid structures show improved properties as compared to the gelatin electrospun mesh. There is no statistical significance between the studied mechanical parameters of Coated and Blend structures which are both stiffer then the Multilayer structure, closely mimicking the native skin mechanical properties. However, the standard deviation associated to the Blend structure can be related to the lack of fiber diameter homogeneity.

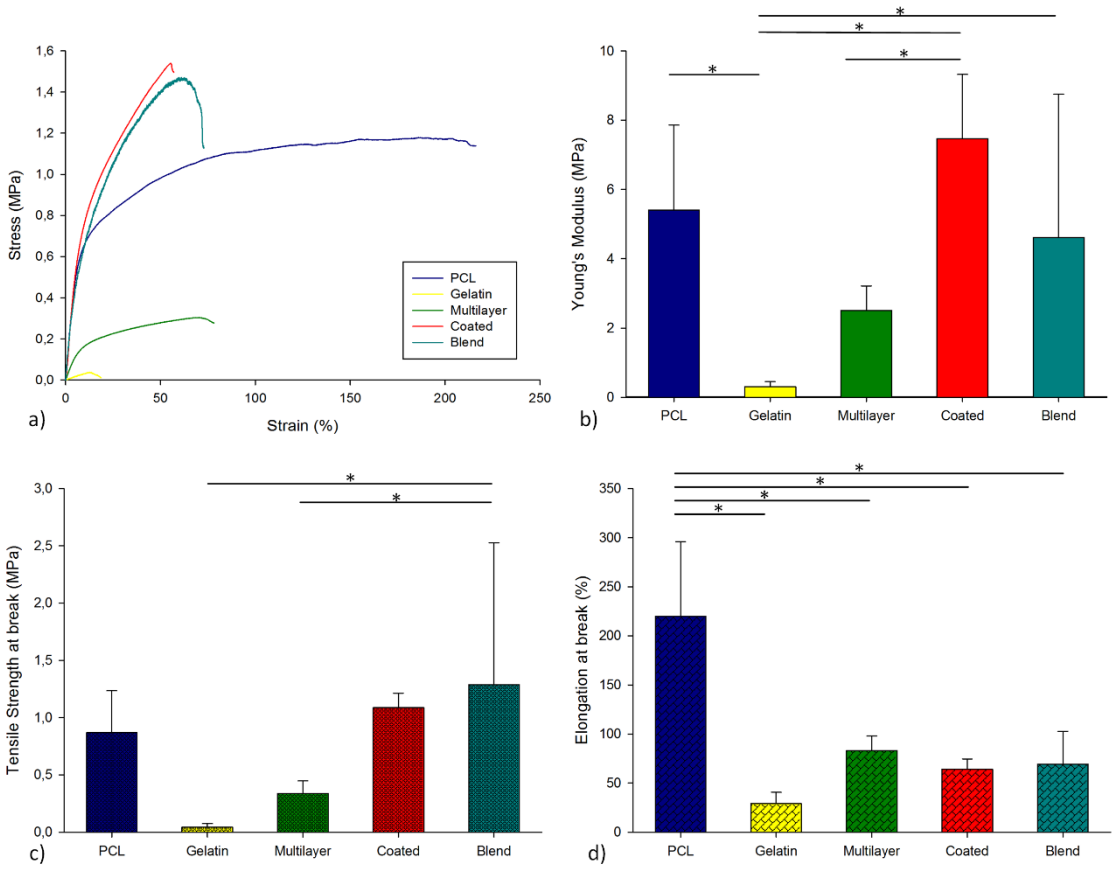

Figure 2. Mechanical behaviour at wet state, a) stress-strain representative curves; b) Young's Modulus, c) Tensile strength at break and d) Elongation at break. Statistical significance for p≤0.05 (*).

3.4 Cytotoxicity

The cytotoxicity of the produced electrospun meshes was performed to the hybrid structures and single structures. According to the results obtained (Fig. 3), fibroblasts remained metabolically active in all conditions tested. In direct contact assay, after 24h, no cytotoxicity was observed for Gel, Multilayer and Coated samples. However, a slight decrease in the metabolic activity of PCL and Blend samples can be correlated with the presence of a small amount of solvent residues into the electrospun mesh. In the indirect assay no sample has present any toxicity.

From all the tested samples, the multilayer structures presented the higher metabolic activity in direct contact and PCL in the indirect contact assay.

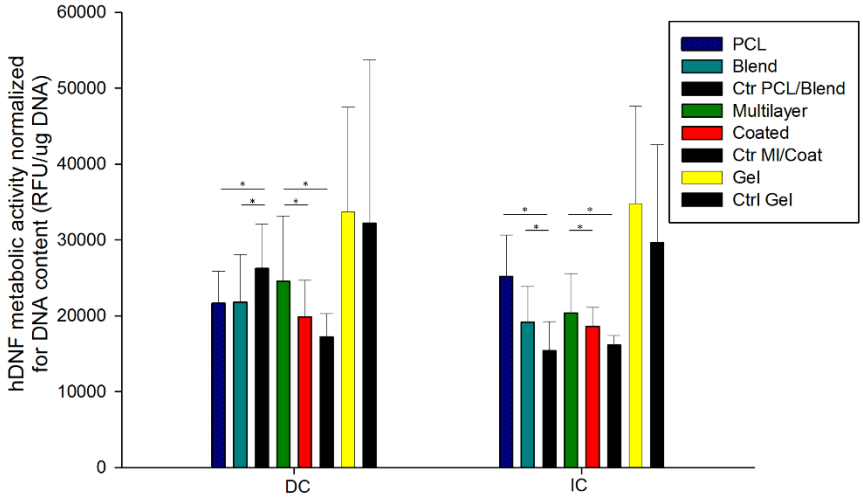

Figure 3. hDNF Metabollic activity normalized for DNA content of different electrospun structures. Statistical significance (*) p≤0.05.

3.5 Cell metabolic activity and proliferation

The proliferation of hDNF during 14 days seeded on electrospun meshes was accessed using the metabolic activity assay (Fig. 4) and cells morphology were further observed by SEM (Fig. 5) and confocal microscopy (Fig. 6 and 7). Throughout the 14

days the cells remained metabolic active and increasing its activity between time-points.

According to the literature PCL does not have affinity to the cells due to its hydrophobic character [56] and on the other hand Gel has many integrin-binding sites and thus can enhance the metabolic activity of cells. So, it is expected that the hybrid structures present better biologic activity than PCL electrospun meshes due the addition of Gel. At day 1 the metabolic activity is low, probably due to the release of any residue of solvent, or cells are still adhering and adapting to the surface of the fires, or some of them lost during the seeding. Though after it the hDNF activity increases consistently over the 14 days with statistical significance as compared with the control. Looking to the results at day 3, PCL presents the lowest activity and Blend the highest, additionally both are statistical different from the other samples. The other approaches present similar results without statistical significance. At day 7 the PCL and Blend presents the same behavior that in the previous time-point. Its notorious that after 7 days of culture the hybrid structures present higher metabolic activity than Gel and this trend is kept up to 14 days. At the end of proliferation assay the hybrid structure with higher activity was the Coated followed by Multilayer and Blend structure. This important result clearly demonstrates that to promote the cell activity is necessary, not only, the adequate biological environment but, also, the appropriate mechanical properties. According to Wells substrate stiffness affect in different ways the cell function, from the most simple point of view stiffness can regulate cell growth, viability and resistance to apoptosis [73]. Moreover, enough scaffold stiffness is crucial for anchorage-dependent cells helping it bonding to the matrix and proliferate [72]. However, the cell migration is commonly associated to an intermediate stiffness level [74]. The coated structure is stiffer than the other hybrid structures and the cells metabolic activity is higher up day 14, corroborate the literature.

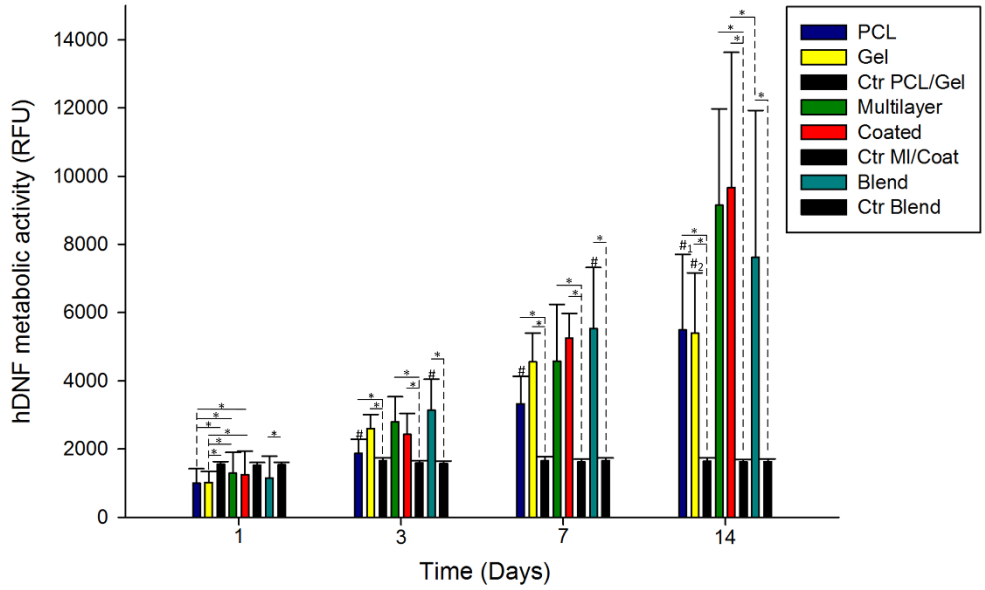

Figure 4. hDNF metabolic activity assay. The control were used electrospun meshes without cells seeded. Statistical significance for p≤0.05 (*) and '#' for statistical significance compared with all other samples, '$\#_1$'except gelatin, '$\#_2$' except PCL.

3.6 Cell morphology, fibronectin deposition and Ki-67 expression

Regarding SEM, after 24h it is possible to observe cells adhered to the nanofibers presenting the typical spindle-like fibroblast morphology, showing a higher degree of spreading with some extended lamellipodia over the surface of all the electrospun structures. Depending on the type of sample it is possible observe different amount of cells there are directly related to the hydrophilic/hydrophobic character of the structure. The seeding was made on the center of the structure but in the hydrophilic structures the seeding is automatically absorbed and the cells are spread around all structure. In the case of hydrophobic surface, the cells take more time to spread across the structure and for that reason the cells density is higher in the center of sample. With time, cells spread across all structures, although, at day 14 the PCL, Multilayer and Coated samples present an uniform film formed with cells at the structure' surface.

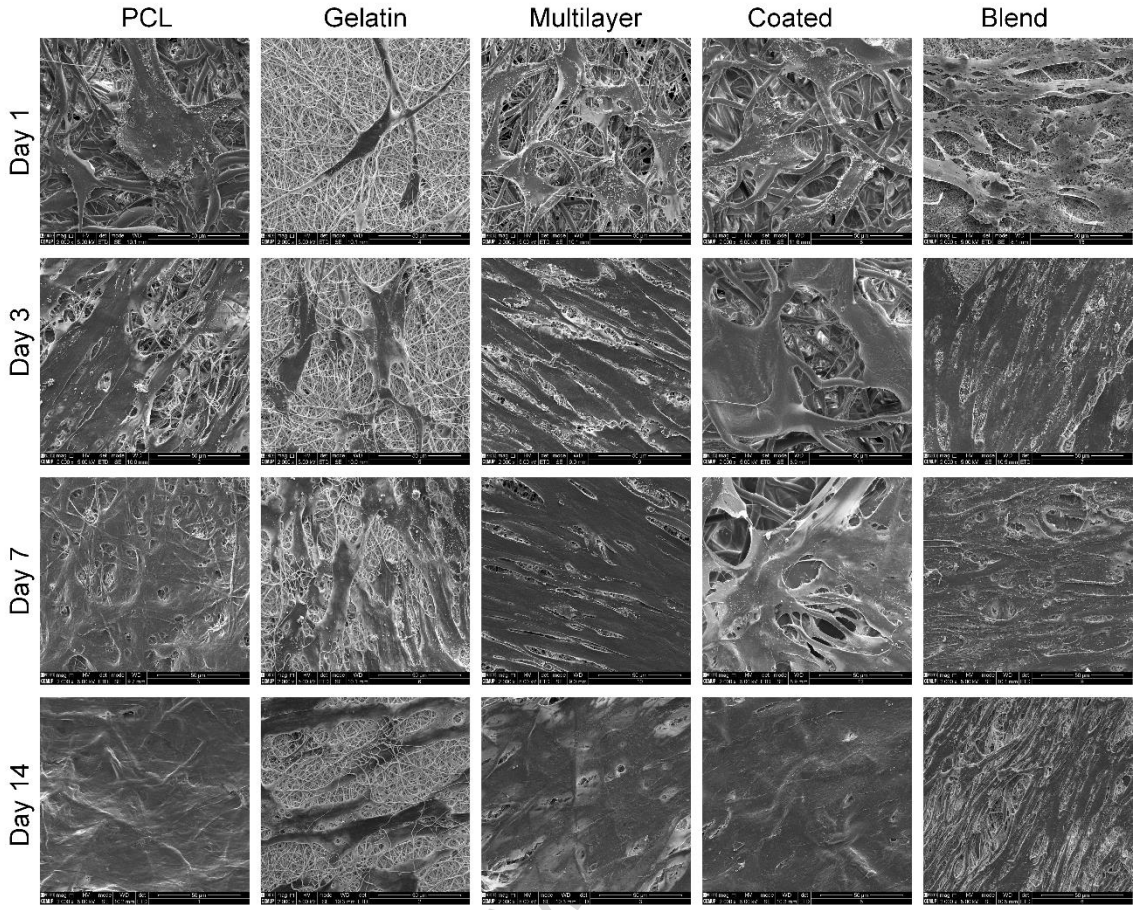

Figure 5. Scanning electron microscopy images representative of hDNF proliferation in different structures over 14 days (Scale bars: 50 µm).

Confocal microscopy was performed at day 1,3, 7 and 14 of culture. Time-points of 1st and 14th day are represented in Figures 6 and 7, respectively. According to the images obtained, all structures present the typical fibroblastic morphology, increasing the number of cells with the culture time, correlating well with SEM observation. FN deposition was explored due to its importance in the wound healing process and the Ki-67 expression was evaluated due to its association to cell proliferation [75, 76]. Regarding to the images at Day 1, it is possible observe in PCL, Gel and Coated structures the interaction between cells. However, only in PCL, Coated and Blend samples have FN deposition in a fibrillary form. In terms of cell proliferation all structures present Ki-67 protein but with highest expression in Gel, Multilayer and Blend structures. After 14 days of culture the presence of cytoskeleton, which provides

a structural framework, facilitates intracellular transport, supports cell junctions and transmits signals about cell contact, adhesion and motility, is lower in the Gel electrospun mesh, probably due to the poor structure stiffness. In the other electrospun meshes a complex cytoskeleton was observed with several cell junctions, forming a network exhibiting cell alignment, mostly in case of the Coated and Blend structures that is common occurs with aligned fibres.

In all structures, the FN has been deposited by the cells in a fibrillar form and comparing with the actin cytoskeleton location indicates that its distribution followed cellular organization. After 14 days the cells on PCL, Gel, Multilayer, Coated and Blend structures continues proliferating, although with higher expression of Ki67 marker in Multilayer structure.

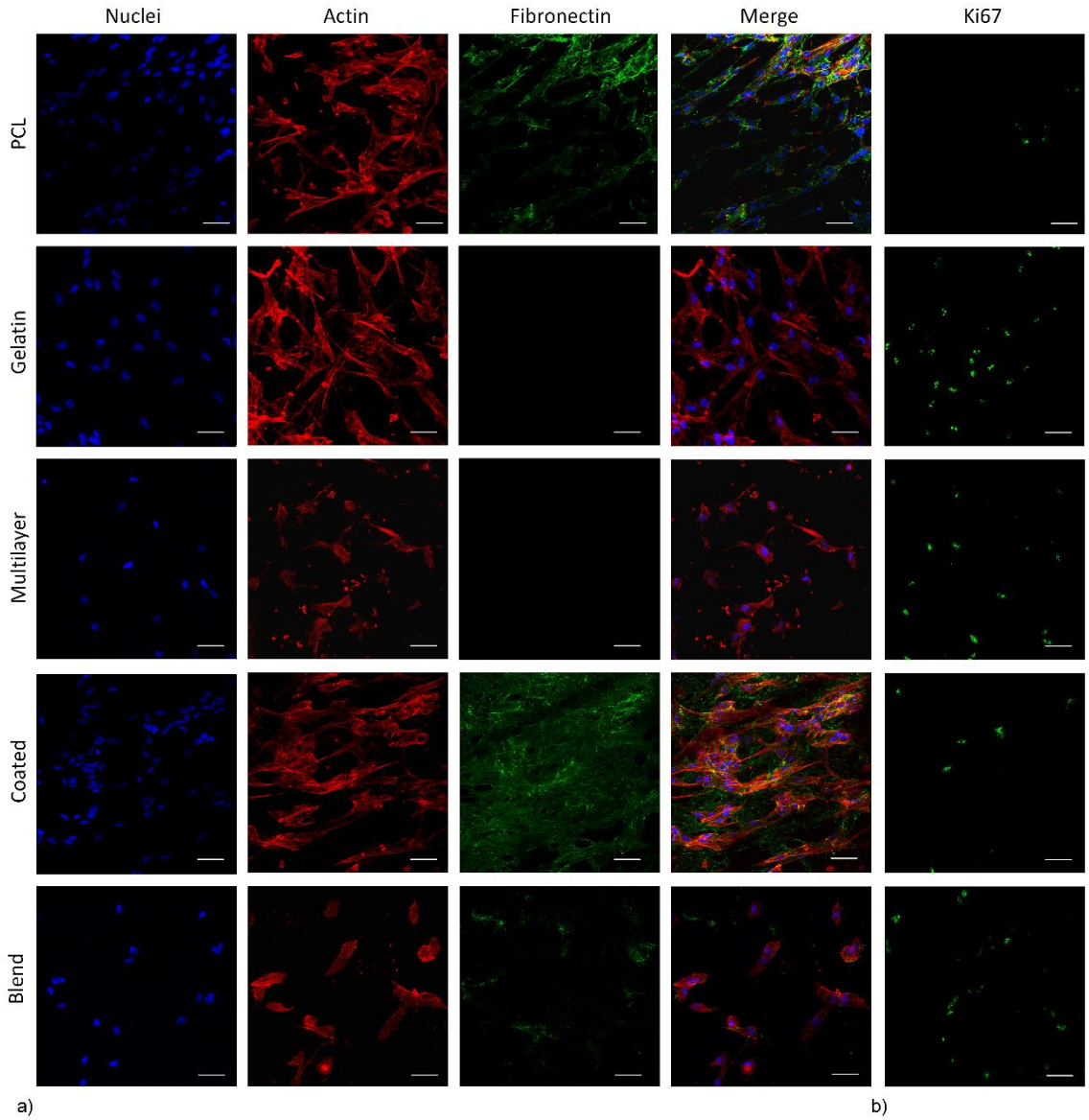

Figure 6. Confocal representative images after 1 day of hDNF culture, a) stained for nuclei (blue), F-actin (red), Fibronectin (green) and b) stained for Ki67 (green) (scale bars: 50µm).

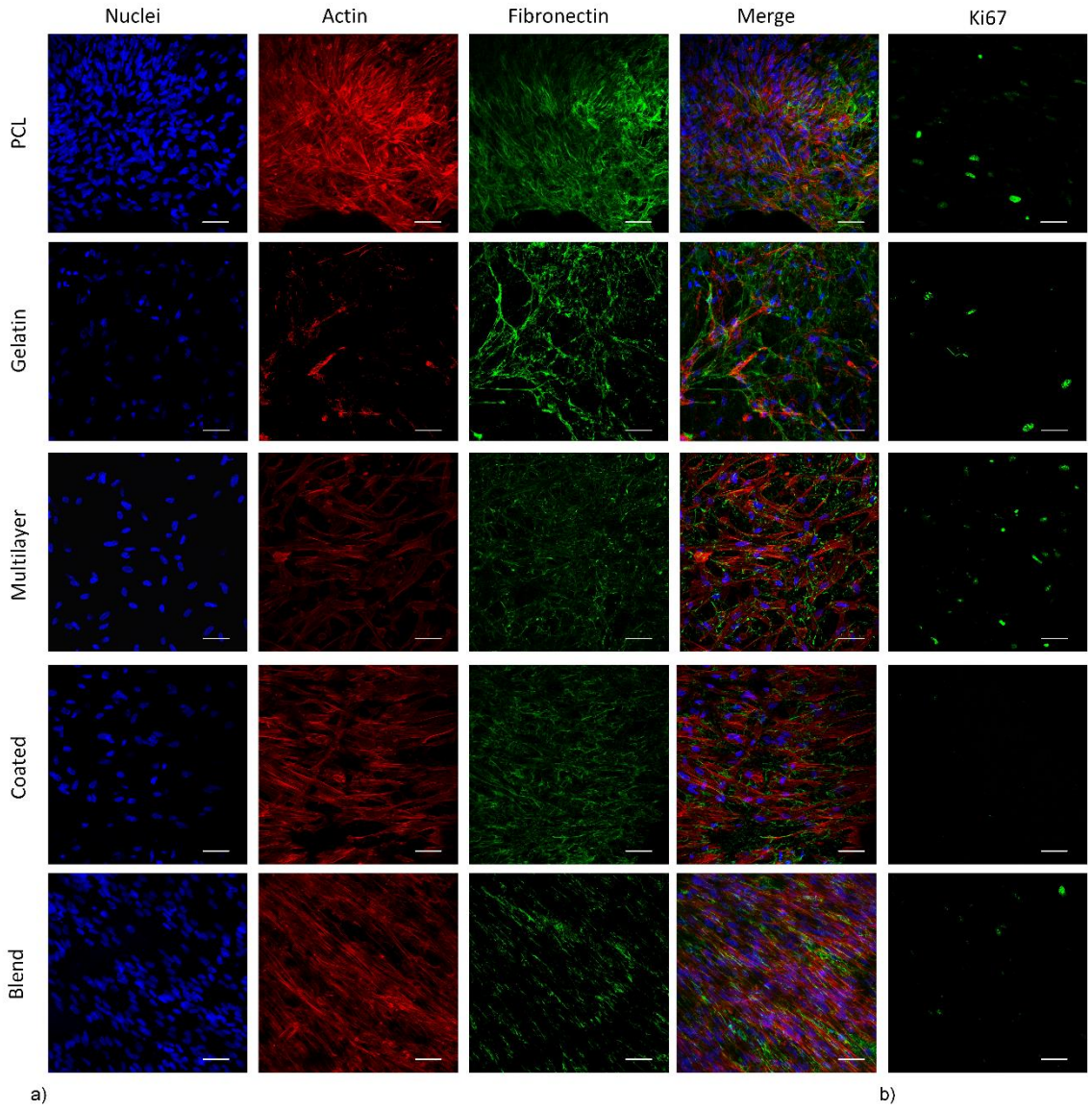

Figure 7. Confocal representative images after 14 day of hDNF culture, a) stained for nuclei (blue), F-actin (red), Fibronectin (green) and b) stained for Ki67 (green) (scale bars: 50µm).

PCL is a well-known biomaterial widely used in tissue engineering applications mostly due to its mechanical properties, although its hydrophobic nature limits its application in biomechanical systems [56]. On the other hand, Gel presents many integrin biddings that are essentials to promote cell adhesion, differentiation and proliferation although presents poor mechanical properties [77]. The development of combined and functional structures has been highlighted as the most promisor strategy to overcome the limitations of each of the materials alone [11]. Most of the published works in the

literature explore the combination of PCL with gelatin as a blend using different ratios and have evaluated the best performing formulation for a specific application [32, 37, 78, 79]. However, most of these studies evaluate the mechanical properties in dry state when final application is in moist environment.

Few works [80, 81] have been exploring the core/shell approach with PCL/Gel or vice-versa. Those studies described that is possible make fibers with well-defined core and shell demonstrating its potential for drug delivery systems and the possibility to tailor the fibers properties according materials concentration.

Planz et al., work evaluated two different approaches (Blend and Multimaterial) and demonstrated that fabricated a structure that mimic the biomechanical characteristics of native ECM in human skin [72]. However, Gel fibers were used as sacrifice material to create a bio-adaptive hybrid structure, degrading into the cell culture medium and increasing the mesh porosity over time [72]. In our work are addressed and compared, for the first time, three different strategies to produce hybrid wound dressings-like structures where PCL and Gel are combined according to different processing approaches (Blend, Multilayer and Coated). The current study demonstrates the impact of using different strategies to combine two widely studied materials into hybrid structures on several properties. This will affect the materials' properties and stability and ultimately the biological performance towards a wound dressing application. The compromise between the physical environments *vs* biochemical cues (adhesion points) is a key factor to favors the cell-matrix interactions.

Furthermore, the hybrid electrospun meshes obtained show different properties and performances being the most promisors the Multilayer and Blend structures. Both have shown to have a great potential as wound dressings due to their ideal water vapor permeability rate, adequate water uptake, hydrophilicity, non-toxicity and capability to promote fibroblasts attachment, proliferation and ECM production (FN). However, multilayer structure presents several advantages compared to Blend structure, namely: i) thicker structure without loss porosity and pores interconnectivity consequence of the

multiple layers composed by different fiber diameters and ii) it is possible handle the structure without damage. Thus, we consider the Multilayer approach ideal to be used as wound dressing.

4. Conclusions

A correlation between the different electrospun hybrid structures using PCL and Gel was addressed in this work, targeting wound dressing applications. Hybrid structures were successfully developed combining the major advantages from individual PCL and Gel electrospun meshes make possible to obtain constructs with good mechanical and biological performance, fitting the requirements to promote an optimal wound healing process. According to the biological assays the use of toxic solvents and crosslinker does not induce any toxicity to the final structures and the hDNF cells can proliferate during 14 days. From the hybrid structures and according all characterization performed the multilayer structure demonstrated to be the most promising strategy to be used as a combined processing route for wound dressing.

Acknowledgements

This study was supported by the Projects PTDC/BBB-ECT/2145/2014 and UID/Multi/04044/2013, financed by European Fonds Européen de Développement Régional (FEDER) through the Portuguese national programs Programa Operacional Factores de Competitividade (COMPETE), Portugal2020 and Norte2020, and by Portuguese funds through Fundação para a Ciência e a Tecnologia (FCT). This work is also supported by the research grants SFRH/BD/91104/2012 awarded to Juliana Dias and SFRH/BPD/90047/2012 awarded to Aureliana Sousa by FCT, and by the Investigator FCT program IF/00411/2013, awarded to Ana L. Oliveira. The authors thanks to CEMUP, University of Porto for the SEM images.

References

[1] C. G., The physiology of the skin, Nursing Standard 16 (2002) 47-51.

[2] T.N. Yildirimer L, Seifalian AM, Skin regeneration scaffolds a multimodal bottom-up approach, Trends Biotechnol 30 (2012) 638-48.
[3] R.S. Reddy VJ, Ravichandran R, Mukherjee S, Balamurugan R, Sundarrajan S, Ramakrishna S., Nanofibrous structured biomimetic strategies for skin tissue regeneration, Wound Rep Reg (2013) 211-16.
[4] M. S., Progress and opportunities for tissue-engineering skin, Nature 445 (2007) 874-80.
[5] L.D. Zhou SS, Zhou YM, Cao JM, The skin function: a factor of anti-metabolic syndrome, Diabetology & Metab Syndrom 4 (2012) 1-11.
[6] M.J. Lai-Cheong JE, . Structure and function of skin, hair and nails, Medicine 41 (2013) 317-20.
[7] Enoch S, Leaper DJ, Basic science of wound healing, Surgery 26 (2007) 31-7.
[8] D.B. Tortora GJ, Principles of Anatomy and Physiology 13th edition, 2012.
[9] R.I. Zahedi P, Ranaei-Sidat SO, Jafari SH, Supaphol P., A review on wound dressings with an emphasis on electrospun nanofibrous polymeric bandages, Polym. Adv. Technol 21 (2009) 77-95.
[10] B.C. Pereira RF, Granja PL, Bártolo PJ. , Advanced biofabrication strategies for skin regeneration and repair, Nanomedicine 8 (2013a) 603-21.
[11] Dias JR, Granja PL, Bártolo PJ, Advances in electrospun skin substitutes, Progress in Materials Science 84 (2016) 314-334.
[12] I.H.L. Pereira, E. Ayres, L. Averous, G. Schlatter, A. Hebraud, S.T.O.L. Mendes, R.L. Oréfice, Elaboration and Characterization of Coaxial Electrospun Poly(ε-Caprolactone)/Gelatin Nanofibers for Biomedical Applications, Advances in Polymer Technology 33(1) (2014).
[13] M. Climent, La primera fábrica del mundo de nanofibras 'bio', El Mundo, 2017.
[14] K.A. Rieger, N.P. Birch, J.D. Schiffman, Designing electrospun nanofiber mats to promote wound healing – a review J. Mater. Chem. B 1 (2013) 4531.
[15] M. Abrigo, S.L. McArthur, P. Kingshott, Electrospun Nanofibers as Dressings for Chronic Wound Care: Advances, Challenges, and Future Prospects, Macromol. Biosci. 14 (2014) 772-792.
[16] R. Augustine, N. Kalarikkal, S. Thomas, Advancement of wound care from grafts to bioengineered smart skin substitutes, Prog Biomater 3 (2014) 103-113.
[17] Grey CP, Newton ST, Bowlin GL, Haas TW, Simpson DG, Gradient fiber electrospinning of layered scaffolds using controlled transitions in fiber diameter, Biomaterials 34(2013) (2013) 4993-5006.
[18] Sundararaghavan HG, Burdick JA, Gradients with Depth in Electrospun Fibrous Scaffolds for Directed Cell Behavior, Biomacromolecules 12(2344-50) (2011).
[19] Abrigo M, Kingshott P, McArthur SL, Electrospun Polystyrene Fiber Diameter Influences Bacterial Attachment, Proliferation and Growth, Appl. Mater. Interfaces 7(14) (2015) 7644-52.
[20] Tijing LD, Ruelo MTG, Amarjargal A, Pant HR, Park CH, K. CS, One-step fabrication of antibacterial (silver nanoparticles/poly(ethylene oxide)) e Polyurethane bicomponent hybrid nanofibrous mat by dual-spinneret electrospinning, Materials Chemistry and Physics 137(2012) (2012) 557-61.
[21] Jin G, Prabhakaran MP, Ramakrishna S, Stem cell differentiation to epidermal lineages on electrospun nanofibrous substrates for skin tissue engineering, Acta Biomaterialia 7(2011) (2011) 3113-22.
[22] Har-el Y-e, Gerstenhaber JA, Brodsky R, Huneke RB, Lelkes PL, Electrospun soy protein scaffolds as wound dressings: Enhanced reepithelialization in a porcine model of wound healing, Wound Medicine 5(2014) (2014) 9-15.
[23] Park SH, Kim MS, Lee BJ, Park JH, Lee HJ, Lee NK, Jeon NL, Suh K-Y, Creation of a hybrid scaffold with dual configuration of aligned and random electrospun fibers, Appl. Mater. Interfaces, (2016) 1-27.
[24] Okamoto M, John B, Synthetic biopolymer nanocomposites for tissue engineering scaffolds, Prog Polym Sci 38(10-11) (2013) 1487-1503.
[25] Dash TK, Konkimalla VB, Poly- e-caprolactone based formulations for drug delivery and Tissue engineering, J. Control. Release 158 (2012) 15-33.
[26] Patricio T, Domingos M, Gloria A, Bartolo P, Characterisation of PCL and PCL/PLA scaffolds for tissue engineering, Procedia CIRP 5 (2013) 110-114.
[27] Gümüşderelioğlu M, Dalkıranoğlu S, Aydın RST, Çakmak S, A novel dermal substitute based on biofunctionalized electrospun PCL nanofibrous matrix, J Biomed Mater Res Part A 98(A) (2011) 461-472.
[28] Joshi JR, Patel RP, Role of Biodegradable Polymers in Drug Delivery, International Journal of Current Pharmaceutical Research 4 (2002) 74-81.
[29] Ige OO, Umoru LE, Aribo S, Natural Products: A Minefield of Biomaterials., International Scholarly Research Network (1-20) (2012).

[30] Sell SA, Wolfe PS, Garg K, McCool JM, Rodriguez IA, Bowlin GL, The Use of Natural Polymers in Tissue Engineering: A Focus on Electrospun Extracellular Matrix Analogues, Polymers 2 (2010) 522-553.
[31] Khan MN, Islam JMM, Khan MA, Fabrication and characterization of gelatin-based biocompatible porous composite scaffold for bone tissue engineering, Biomed Mater Res Part A 100 (2012) 3020-3028.
[32] Gautam S, Dinda AK, Mishra NC, Fabrication and characterization of PCL/gelatin composite nanofibrous scaffold for tissue engineering applications by electrospinning method, Materials Science and Engineering C 33(1228-1235) (2013).
[33] Nagiah N, Madhavi L, Anitha R, Anandan C, Srinivasan NT, Sivagnanam UT, Development and characterization of coaxially electrospun gelatine coated poly (3-hydroxybutyric acid) thin films as potential scaffolds for skin regeneration, Materials Science and Engineering C 33 (2013) 4444-4452.
[34] Zhan J, Lan P, The Review on Electrospun Gelatin Fiber Scaffold, Journal of Research Updates in Polymer Science 1 (2012) 59-71.
[35] Panzavolta S, Gioffrè M, Focarete ML, Gualandi C, Foroni L, Bigi A, Electrospun gelatin nanofibers: Optimization of genipin cross-linking to preserve fiber morphology after exposure to water, Acta Biomaterialia 7 (2011) 1702-1709.
[36] M.-K. Yeh, Y.-M. Liang, K.-M. Cheng, N.-T. Dai, C.-C. Liu, J.-J. Young, A novel cell support membrane for skin tissue engineering: Gelatin film cross-linked with 2-chloro-1-methylpyridinium iodide, Polymer (52) (2011) 996-1003.
[37] Y. Zhang, H. Ouyang, C.T. Lim, S. Ramakrishna, Z.-M. Huang, Electrospinning of Gelatin Fibers and Gelatin/PCL Composite Fibrous Scaffolds, Journal of Biomedical Materials Research Part B Applied Biomaterials (2005) 156-165.
[38] J.R. Dias, S. Baptista-Silva, C.M.T.d. Oliveira, A. Sousa, A.L. Oliveira, P.J. Bártolo, P.L. Granja, In situ crosslinked electrospun gelatin nanofibers for skin regeneration, European Polymer Journal 95 (2017) 161-173.
[39] J.R. Dias, C.d. Santos, J. Horta, P.L. Granja, P.J. Bártolo, A new design of an electrospinning apparatus for tissue engineering applications, International Journal of Bioprinting 2(2) (2017) 1-9.
[40] Y.Z. Zhang, J. Venugopal, Z.M. Huang, C.T. Lim, S. Ramakrishna, Crosslinking of the electrospun gelatin nanofibers, Polymer 47 (2006) 2911–2917.
[41] W. He, Z. Ma, T. Yong, W.E. Teo, S. Ramakrishna, Fabrication of collagen-coated biodegradable polymer nanofiber mesh and its potential for endothelial cells growth, Biomaterials (26) (2005) 7606–761.
[42] I. ASTM, Standard test methods for water vapor transmission of materials, E96/E96M-10.
[43] R.C. Team, R: A language and environment for statistical computing., Vienna, Austria, 2014.
[44] Z.Y. Cui W, Chang J, Electrospun nanofibrous materials for tissue engineering and drug delivery, Sci. and technol. Adv. Mater. (2010) 11014108.
[45] P.-M.B. Pramanik S, Osman NAA, Progress if key strategies in development of electrospun scaffolds: bone tissue, Sci. Technol. Adv. Mater. (2012) 131-13.
[46] T.S. Liu W, Xia Y., Electrospun nanofibres for regenerative medicine, Adv. Healthcare Mater 1 (2012) 10-25.
[47] Molly MS, Juliana HG, Exploring and engineering the cell surface interface, Science (310) (2005) 1135-1138.
[48] Sun T, Norton D, McKean RJ, Haycock JW, Ryan AJ, MacNeil S, Development of a 3D Cell Culture System for Investigating Cell Interactions With Electrospun Fibers, Biotechnology and Bioengineering 97(5) (2007) 1318-1328.
[49] N. Cebi, M.Z. Durak, O.S. Toker, O. Sagdic, M. Arici, An evaluation of Fourier transforms infrared spectroscopy method for the classification and discrimination of bovine, porcine and fish gelatins, Food Chemistry 190 (2016) 1109–1115.
[50] M. Nagarajan, S. Benjakul, T. Prodpran, P. Songtipya, H. Kishimura, Characteristics and functional properties of gelatin from splendid squid (Loligoformosana) skin as affected by extraction temperatures, Food Hydrocolloids 29 (2012) 389–397.
[51] D. Hashim, M.Y. Che, R. Norakasha, M. Shuhaimi, Y. Salmah, Z. Syahariza, Potential use of Fourier transform infrared spectroscopy for differentiation of bovine and porcine gelatins, Food Chemistry 118 (2010) 856–860.
[52] J.F. Martucci, J.P. Espinosa, R.A. Ruseckaite, Physicochemical properties of films based on bovine gelatin cross-linked with 1,4-butanediol diglycidyl ether, Food Bioprocess Technol (8) (2015) 1645-1656.
[53] R. Núñez-Flores, B. Giménez, F. Fernández-Martín, M.E. López-Caballero, M.P. Montero, M.C. Gómez-Guillén, Physical and functional characterization of active fish gelatin films incorporated with lignin, Food Hydrocolloids 39 (2013) 243–250.

[54] J. Bandekar, Amide modes and protein conformation, Biochimica et Biophysica Acta: Protein Structure and Molecular Enzymology 1120 (1992) 123–143.
[55] Azevedo HS, Reis RL, Understanding the enzymatic degradation of biodegradable polymers and strategies to control their degradation rate, in: Reis RL, San Roman J (Eds.), iodegradable Systems in Tissue Engineering and Regenerative Medicine, CRC Press, Boca Raton, FL, 2005, pp. 177-201.
[56] A. Cipitria, A. Skelton, T. Dargaville, D. Daltonac, D. Hutmacher, Design, fabrication and characterization of PCL electrospun scaffolds—a review, J. Mater. Chem., 2011, 21, 9419 21 (2011) 9419.
[57] Q. Xing, K. Yates, C. Vogt, Z. Qian, M.C. Frost, F. Zhaoa, Increasing Mechanical Strength of Gelatin Hydrogels by Divalent Metal Ion Removal, Sci Rep. 4 (2014) 4706.
[58] S.-Y. Gu, Z.-M. Wang, J. Ren, S.-Y. Zhang, Electrospinning of gelatin and gelatin/poly(L-lactide) blend and its characteristics for wound dressing Materials Science and Engineering C 29 (2009) 1822–1828.
[59] C.K. Field, M.D. Kerstein, Overview of wound healing in a moist environment, The American Journal of Surgery 16(1A (SUPPL)) (1994) 2-6.
[60] M. Abrigo, S.L. McArthur, P. Kingshott, Electrospun Nanofibers as Dressings for Chronic Wound Care: Advances, Challenges, and Future Prospects, Macromol. Biosci. 14 (2014) 772-792.
[61] L.O. Lamke, G.E. Nilsson, H.L. Reithner, The evaporative water loss from burns and the water-vapour permeability of grafts and artificial membranes used in the treatment of burns, Burns 3(3) (1977) 159-165.
[62] R. Dave, H.M. Joshi, V.P. Venugopalan, Biomedical evaluation of a novel nitrogen oxides releasing wound dressing, J Mater Sci: Mater Med 23 (2012) 3097–3106.
[63] S. Gustaitea, J. Kazlauskea, J. Bobokalonova, S. Perni, V. Dutschkc, J. Liesienea, P. Prokopovich, Characterization of cellulose based sponges for wound dressings, Colloids and Surfaces A: Physicochem. Eng. Aspects 480 (2015) 336–342.
[64] M.M. Hohmann, M. Shin, G. Rutledge, M.P. Brenner, Electrospinning and electrically forced jets I stability theory, Phys. Fluid. (13) (2001) 2201–2220.
[65] H.S. Azevedo, M.G. Francisco, R.L. Reis, In Vitro Assessment of the Enzymatic Degradation of Several Starch Based Biomaterials, Biomacromolecules 4 (2003) 1703-1712.
[66] H. Vogel, Age dependence of mechanical and biochemical properties of human skin, Bioengineering and the skin 3(67-91) (1987).
[67] L. Jansen, P. Rottier, Some mechanical properties of human abdominal skin measured on excised strips, Dermatologica 117 (1985) 65-83.
[68] C. Jacquemoud, K. Bruyere-Garnier, M. Coret, Methodology to determine failure characteristics of planar soft tissues using a dynamic tensile test, Journal of Biomechanics 40(2) (2007) 468-475.
[69] J.-f. Pan, N.-H. Liu, H. Sun, F. Xu, Preparation and Characterization of Electrospun PLCL/Poloxamer Nanofibers and Dextran/Gelatin Hydrogels for Skin Tissue Engineering, PLoS ONE 9(11) (2014) e112885.
[70] Y. Yin, D. Pu, J. Xiong, Analysis of the comprehensive tensile relationship in electrospun silk fibroin/polycaprolactone nanofiber membranes. Membranes, Membranes 7(67) (2017) 1-14.
[71] A. Butcher, M. Oyen, Mechanical properties of electrospun gelatin scaffolds, Front. Bioeng. Biotechnol. (2016).
[72] V. Planz, S. Seif, J.S. Atchison, B. Vukosavljevic, L. Sparenberg, E. Kroner, M. Windbergs, Three-dimensional hierarchical cultivation of human skin cells on bio-adaptive hybrid fibers, Integr. Biol. 8 (2016) 775-784.
[73] R.G. Wells, The Role of Matrix Stiffness in Regulating: Cell Behavior, Hepatology 47(4) (2008) 1394-1399.
[74] D.E. Discher, P. Janmey, Y.-l. Wang, Tissue Cells Feel and Respond to the Stiffness of Their Substrate, Science 310 (2005) 1139-1143.
[75] A. Hielscher, K. Ellis, C. Qiu, J. Porterfield, S. Gerecht, Fibronectin Deposition Participates in Extracellular Matrix Assembly and Vascular Morphogenesis. , PLoS ONE 11(1) (2016) e0147600.
[76] T. Scholzen, J. Gerdes, The Ki-67 Protein: From the Known and the Unknown, Journal of Cellular Physiology 182 (2000) 311–322
[77] G. Jin, Y. Li, M.P. Prabhakaran, W. Tian, S. Ramakrishna, In vitro and in vivo evaluation of the wound healing capability of electrospun gelatin/PLLCL nanofibers, Journal of Bioactive and Compatible Polymers 29(6) (2014) 628–645.
[78] R. Zheng, H. Duan, J. Xue, Y. Liu, B. Feng, S. Zhao, Y. Zhu, Y. Liu, A. He, W. Zhang, W. Liu, Y. Cao, G. Zhou, The influence of Gelatin/PCL ratio and 3-D construct shape of electrospun membranes on cartilage regeneration, Biomaterials 35 (2014) 152-164.

[79] R. Yao, J. He, G. Meng, B. Jiang, F. Wu, Electrospun PCL/Gelatin composite fibrous scaffolds: mechanical properties and cellular responses, Journal of Biomaterials Science, Polymer Edition 27(9) (2016) 824-838.
[80] M. He, J. Xue, H. Geng, H. Gu, D. Chen, R. Shi, L. Zhang, Fibrous guided tissue regeneration membrane loaded with anti-inflammatory agent prepared by coaxial electrospinning for the purpose of controlled release, Surface Science (2015).
[81] M. Gulfam, J.M. Lee, J.-e. Kim, D.W. Lim, E.K. Lee, B.G. Chung, Highly Porous Core Shell Polymeric Fiber Network, Langmuir 27 (2011) 10993–10999.

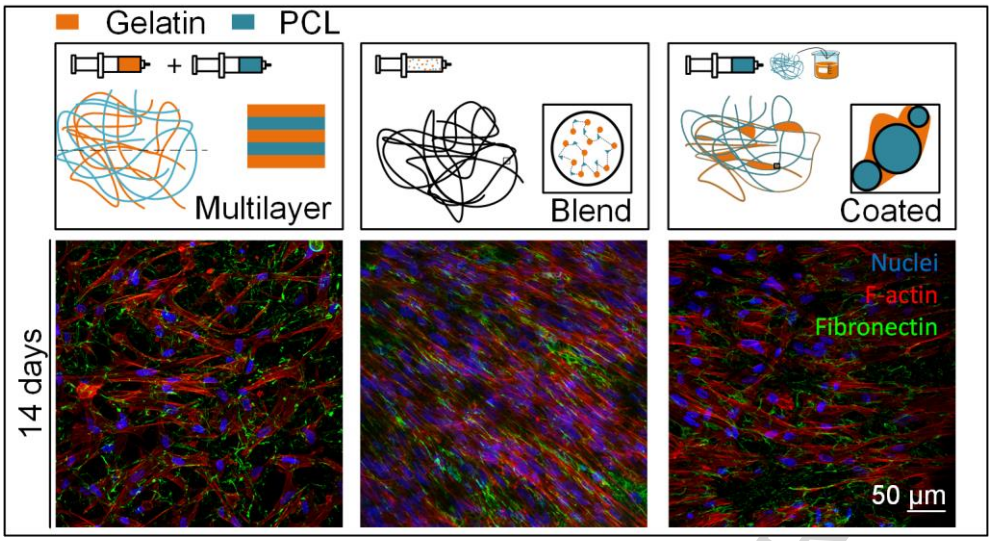

Graphical abstract

Highlights

- Processing strategies allows to generate biomimetic and complex structures.
- Hybrid structures that mimic the skin ECM properties were developed.
- Processing strategies shape the final structure properties;
- Structure mechanical strength have a direct correlation on cellular adhesion;
- Multilayer stood out due to its 3D shape and biomechanical properties.